Acta Polytechnica **59**(4):352–358, 2019
DOI:10.14311/AP.2019.59.0352

available online at https://ojs.cvut.cz/ojs/index.php/ap

THE CHARACTERISTICS OF Al-Si COATING ON STEEL 22MnB5 DEPENDING ON THE HEAT TREATMENT

Marie Kolaříková[a,*], Rostislav Chotěborský[b], Monika Hromasová[c], Miloslav Linda[c]

[a] *Czech Technical University in Prague, Faculty of Mechanical Engineering, Department of Manufacturing Technology, Technická 4, 166 07 Prague 6, Czech Republic*

[b] *Czech University of Life Science Prague, Faculty of Engineering, Department of Material Science and Manufacturing Technology, Kamýcká 129, 165 00 Prague 6, Czech Republic*

[c] *Czech University of Life Science Prague, Faculty of Engineering, Department of Electrical Engineering and Automation, Kamýcká 129, 165 00 Prague 6, Czech Republic*

[*] corresponding author: marie.kolarikova@fs.cvut.cz

Abstract. The coating on the 22MnB5 steel is intended to protect it against oxidation during the forming process. This steel is hot-pressed. A preheating before the pressing and subsequent hardening in the tool affects the properties of the AlSi coating. This study summarizes the results of investigating the effect of heat treatment parameters on the formation of intermetallics in the AlSi coating. The chemical analysis of the coating was performed by the EDX and EBSD method and the mechanical properties were determined by the Hysitron TI 950 TriboIndenter™ system. The result of this study is that, due to a diffusion during the heat treatment, the brittle coating was transformed into a tougher phase.

Keywords: Al-Si coating, intermetallic phase, heat treatment, steel 22MnB5.

1. Introduction

Nowadays, high-strength martensitic hot-formed steels are used for the body stiffening. Their use for bodywork (especially for safety components) is on the rise worldwide. For example, in the Octavia III model, the proportion of high-strength hot-formed steels in 2012 was 26.1 %. Today, there is no car manufacturer, who does not use the sheet metal with a surface treatment when making a bodywork. The primary function of the coatings is to prevent corrosion and thus increase the service life of the bodywork. Furthermore, it improves the surface morphology for a better adhesion of the lubricant required for the forming operations.

An AlSi-based coating on 22MnB5 steel is designed to protect it against oxidation during the forming process. A preheating of the steel before the pressing and subsequent hardening in the tool affects the properties of the AlSi coating. Typically, the Al-Si coating has a nominal thickness of 30-50 μm. The basic composition is 90 % Al + 10 % Si with Si enriched locally. The interlayer at the interface with the steel substrate formed by the heat treatment (forming process) has a thickness of 5 to 10 μm, according to the manufacturer. Its basic constituents are FeAl and Fe_2Al_5 phases. While the Al-Si coating has a melting point of 650-700 °C, FeAl and Fe_2Al_5 have a higher melting point of about 1150-1350 °C. [1–3]

In the delivered state, the Al-Si coating on the ferritic-pearlitic steel is comprised of a compact Al layer with Si precipitates. Upon raising the temperature to an austenitizing temperature during the forming process, Fe begins to diffuse into the Al-Si layer. A tertiary Al-Si-Fe alloy is formed, which gives the coating characteristics. In his work, Grauer et al. [4] accentuates that, at the aluminium melting temperatures (660 °C), the iron diffusion always occurs in the AlSi coating, although the coating is heated very slowly. Windmann [5, 6] describes the dependence of the morphology of the AlSi coating on the heat treatment parameters, and, in this context, the research by Füssela et al. [7] shows that different layer thicknesses significantly change the weldability of the base material. [8–10]

Schmidová et al. [11] examined heat treated AlSi coatings in the temperature range of 880-850 °C with a holding time of 5 - 10 min. This has confirmed the creation of a diffusion layer formed during the heat treatment. Her study shows that the heterogeneous iron enriched in the coating also increases with the temperature and the holding time. The layer with the increasing ratio of Al/Si is formed just below the surface of the coating. The formation of a continuous secondary intermetallic interlayer in a coating with predominantly Al has a particular effect on weldability. Especially in connection with the increasing porosity (Kirkendall's pores) and oxide content on the surface. The higher amount of pores leads to their accidental collapse, which affects the flow and causes an instability of the whole process. According to the study, the maximum thickness of the diffusion layer at the interface of the steel coating is 13 μm. A higher thickness

of the diffusion layer leads to a random occurrence of an instability in the welding process.

Cheng et al. [12] and Springer et al. [13] studied the phase formation at the soft steel interface and AlSi coating (with a silicon concentration of 5 and 10 %) at temperatures of 650-700 °C. They observed the formation of a multilayer phase with the sequence Al_5Fe_2-$Al_{13}Fe_4$-Al_8Fe_2Si, which was formed directly on the steel-coating interface. In addition, they proved the formation of small precipitates of the $Al_2Fe_3Si_3$ type within the Al_5Fe_2 phase. They claim that the silicon has inhibitory effects on the intermetallic growth in the steel-coating interface and that it neutralizes the $Al_{13}Fe_4$ phase formation and it promotes a growth of Al_8Fe_2Si. Their results are consistent with Windmann's work and confirm the work of Yun et al. [14]. Eggeler et al. [15] proved that silicon occupies free positions in the Al_5Fe_2 grid and thus prevents the growth of this phase.

In his next work, Windmann et al. [5] concluded that the iron diffusion from steel to AlSi coating prevails during the first two minutes of the heating (around 900 °C). After two minutes, when aluminium diffuses into the steel, the Al content in the coating decreases and the Al ($Al_{13}Fe_4$ and Al_5Fe_2) rich intermetallic phases are converted to a Fe (AlFe) type. The aluminium-to-steel diffusion supports the formation of an alpha-Fe layer at the interface between the coating and the steel. This layer increases its thickness with the austenitizing temperature and with a temperature-holding time.

Köster et al. [16] as well as Kobayashi et al. [17] found that, in particular, Al_xFe_y -rich Al intermetallic phases (type $Al_{13}Fe_4$ and Al_5Fe_2), which are formed in the AlSi coating, have a low fracture toughness (1 MPa·m$^{1/2}$), which is attributed to their high hardness of 900-1150 HV0.05. According to Krasnowski et al. [18], the hardness of the Al_5Fe_2 phase is 851 HV1. The AlFe and $AlFe_3$ phases have a lower hardness of 300 to 650 HV0.05 (Kubošová et al. [19]) and a higher fracture toughness of up to 26 MPa·m$^{1/2}$. With respect to the stoichiometry of these intermetallics, the the Al_xFe_y phases are tougher and softer and they have a higher Fe content, so they can be stabilized by various diffusion processes. Kim et al. [20] found out that the brittle intermetallic phases of the $Al_{13}Fe_4$ and Al_5Fe_2 types reduced the weldability. According to Shiota et al. [21] the Al_2Fe_3 phase has a hardness of 882 HV1, fracture toughness of 1.6 MPa·m$^{1/2}$ and a modulus of elasticity of 245 GPa.

Our aim is to point out the change of phases into the Al-Si coating of 22MnB5 so that our results could be used for a future research of the weldability of these coated steel. The aim of the research is to help to clarify what is happening in the coating during the heat treatment in terms of a phase formation and mechanical properties and to determine how this influences the weldability and stability of the welding process. The result will be the determination of the thermal processing parameter limits so that changes in the coating affect the process stability as little as possible.

2. Materials and methods

A high-strength boron steel 22MnB5 was chosen as the material for the experiment. 1.2 mm thick sheets were supplied with an AlSi coating. The chemical composition of the 22MnB5 steel is shown in Table 1. The mechanical properties are in Table 2. These materials are supplied from the mills in a cold or hot-rolled condition with a ferritic-perlite structure and eliminated carbides. In this state, the yield strength is $R_{p0.2}$ 350-550 MPa, the strength of R_m is 500-700 MPa and the ductility A80 is greater than 15 %.

For the chemical analysis of all coatings, the MIRA3 GMU scanning electron microscope and the EDS and EBSD analysers from Oxford instruments were used. From the measured data, an elemental map was compiled. Two line profiles have been marked on each map and spot analysis were performed at the selected locations to determine the percentage representation of the elements. At the same time, another measurement was performed by Electron Spectrum Diffraction (EBDS). The Hysitron TI 950 TriboIndenter™ nanoindentation system was used to analyse the mechanical properties of coatings, such as reduced elastic modulus and indentation hardness (HIT, according to ISO 14577-1). Unlike Martens hardness (HM), HIT calculates the contact area (H = F/Acont), Acont as the surface projection (or tip cut) at the maximum contact depth. The XPM (Ultra-Fast Nanoindentation) mode with a maximum load force $P_{max} = 3000\,\mu$N was used for the mechanical analysis, corresponding to the contact depths of $h_c \sim 60 - 100$ nm. The indent matrix 8×30 was separated by 3 μm between individual indents. The load function had two segments: 1st in 1 second load to $P_{max} = 3000\,\mu$N, 2nd in 1 second relieving segment (a tip extraction from sample). The measurement method is described in [22], including the evaluation method.

3. Experiment

Samples were heat treated with various parameters in the range: time t = 5 to 15 min, temperature $T = 850 - 950$ °C. The heat treatment was performed in an induction furnace. The set temperature was verified by the thermocouple and recorded by the ALMENO station.

All samples were analysed for the mechanical properties. The measured values of reduced modulus and indentation hardness were composed into matrices for a better visualization of the results. A chemical analysis followed. This was done at the site of the previous analysis of mechanical properties in order to relate the results to one another. The results of both analyses are shown in Figure 1 - Figure 8.

For clarity, only 4 samples were selected for the comparison: sample 1 without heat treatment, low

C	Si	Mn	P	S	Al	B	Cr	Mo	Ti
0.26	0.30	1.14	0.0075	< 0.150	0.04	0.0027	0.16	0.01	0.032

TABLE 1. Chemical composition of steel 22MnB5.

Before heat treatment			After heat treatment		
$R_{p0,2}$ [MPa]	R_m [MPa]	A_{80} min. [%]	$R_{p0,2}$ [MPa]	R_m [MPa]	A_{80} min. [%]
min 200	400 - 570	15	950 - 1250	1300 - 1650	4.5

TABLE 2. Mechanical properties of steel 22MnB5 .

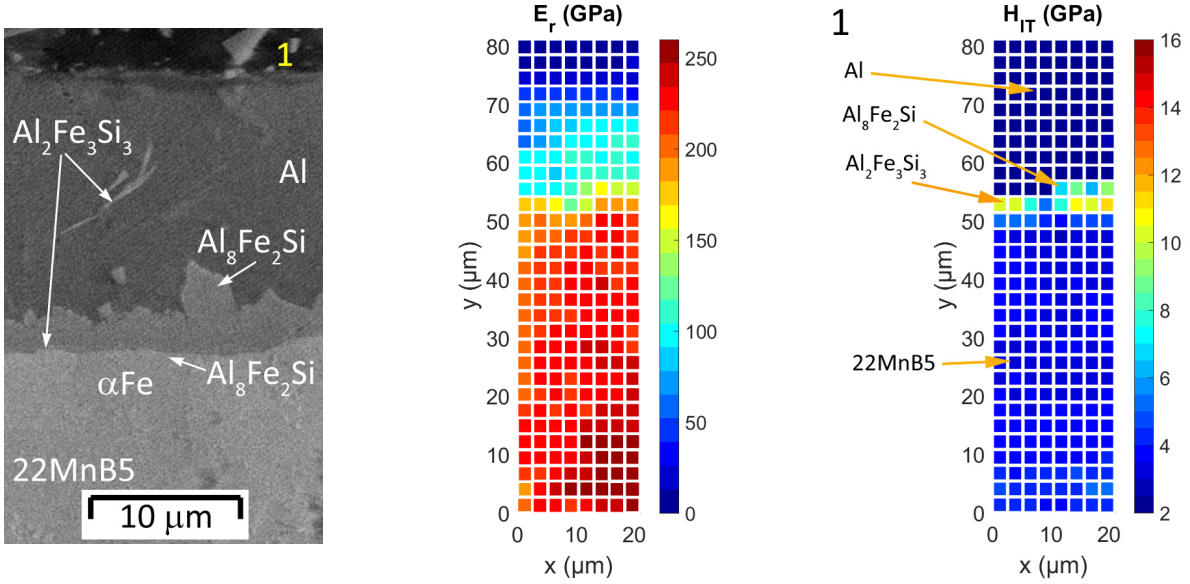

FIGURE 1. Phase identification (left), reduced modulus (center) and indentation hardness (right) of sample 1 before heat treatment.

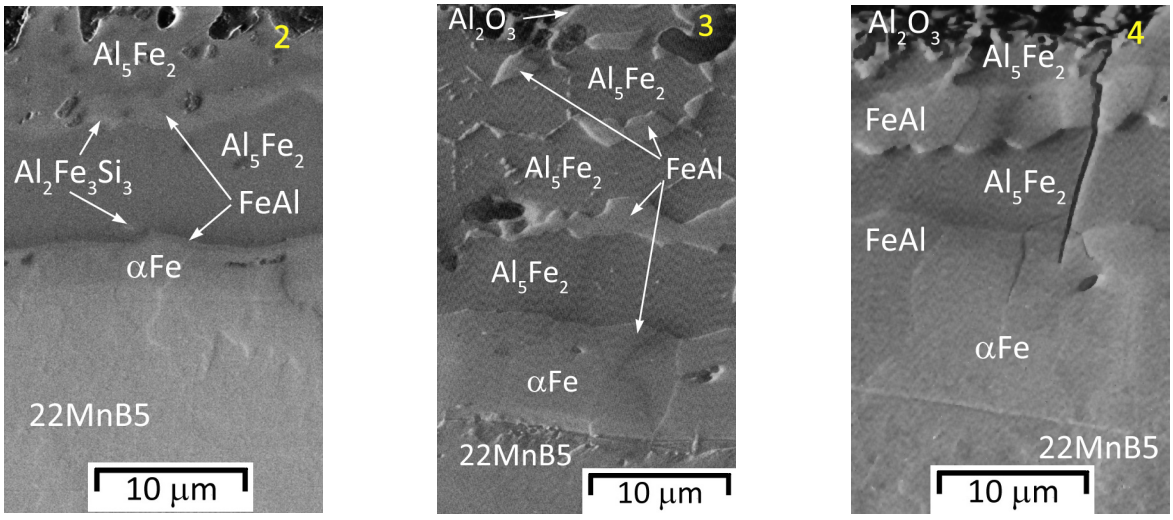

FIGURE 2. Phase identification for samples with heat treatment parameters: time $t = 5.8$ min and temperature $T = 882\,°C$ (2 - left), $t = 7.4$ min and $T = 905\,°C$ (3 - center) and $t = 12.9$ min and $T = 907\,°C$ (4 - right).

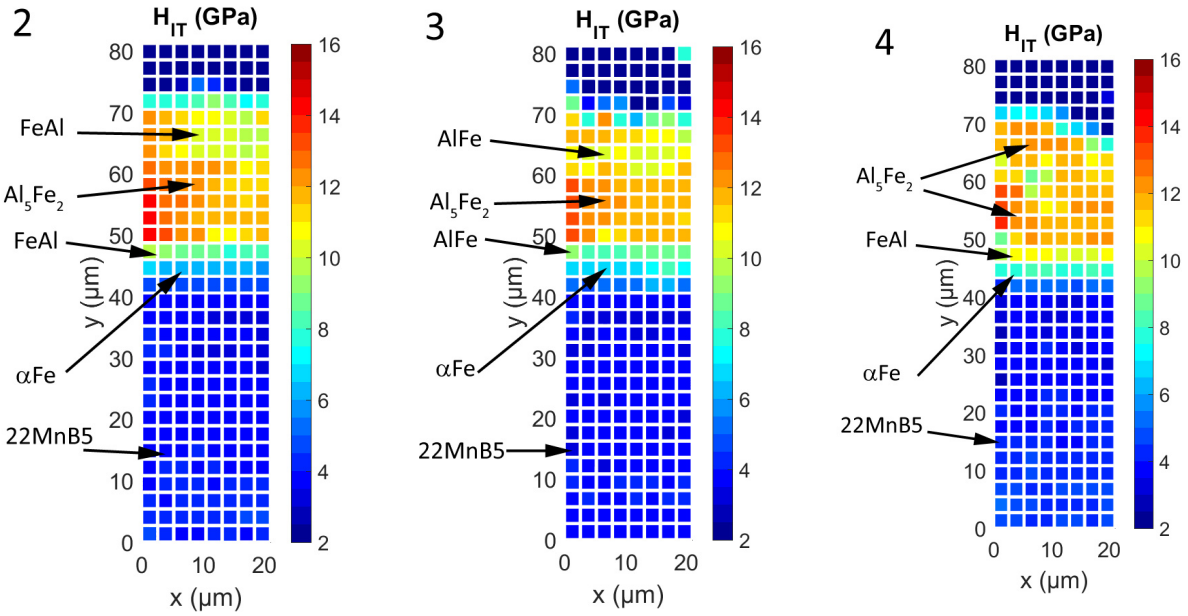

FIGURE 3. Indentation Hardness for samples with heat treatment parameters: time $t = 5.8$ min and temperature $T = 882\,^{\circ}\mathrm{C}$ (left), $t = 7.4$ min and $T = 905\,^{\circ}\mathrm{C}$ (center) and $t = 12.9$ min and $T = 907\,^{\circ}\mathrm{C}$ (right).

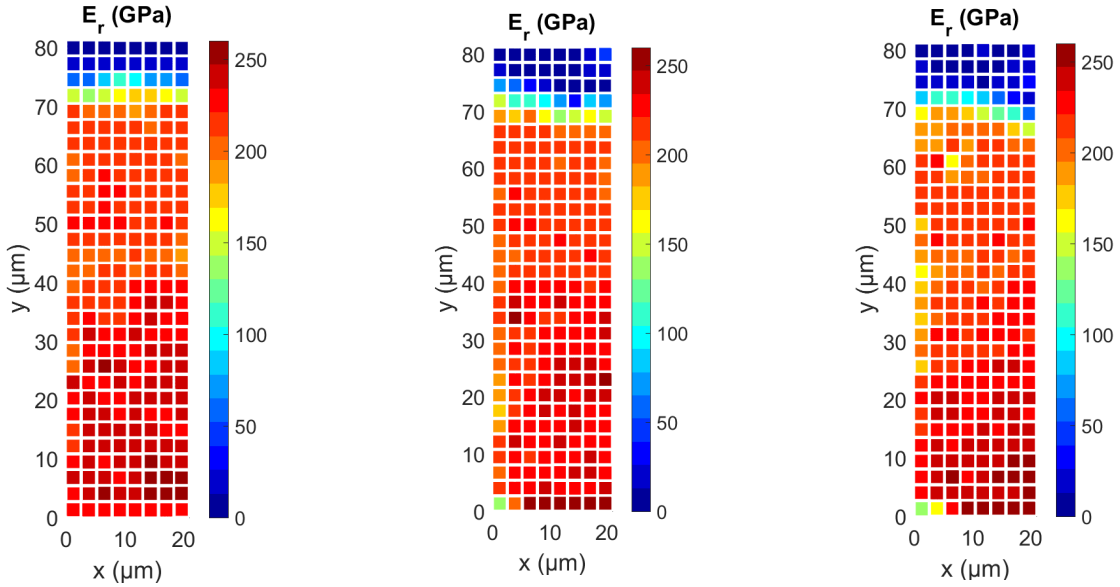

FIGURE 4. Reduced modulus for samples with heat treatment parameters: time $t = 5.8$ min and temperature $T = 882\,^{\circ}\mathrm{C}$ (left), $t = 7.4$ min and $T = 905\,^{\circ}\mathrm{C}$ (center) and $t = 12.9$ min and $T = 907\,^{\circ}\mathrm{C}$ (right).

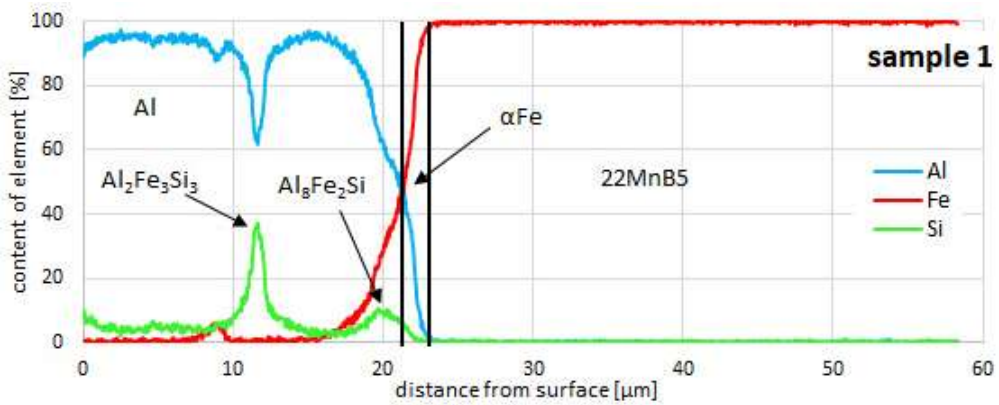

FIGURE 5. Chemical compound in line for sample 1 without heat treatment.

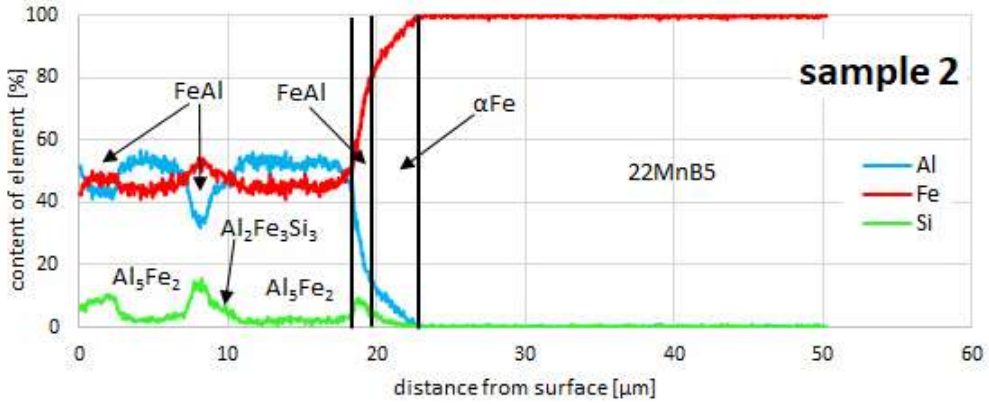

FIGURE 6. Chemical compound in line for sample 2 time ($t = 5.8\,\text{min}$, $T = 882\,°\text{C}$).

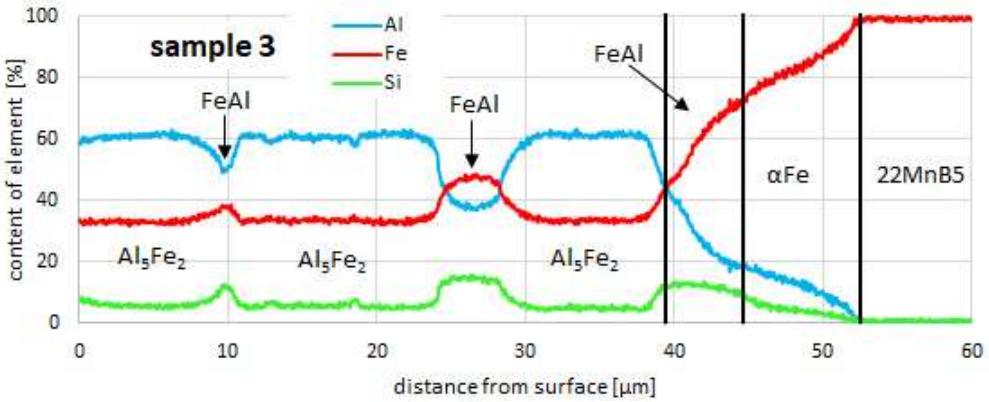

FIGURE 7. Chemical compound in line for sample 3 ($t = 7.4\,\text{min}$, $T = 905\,°\text{C}$).

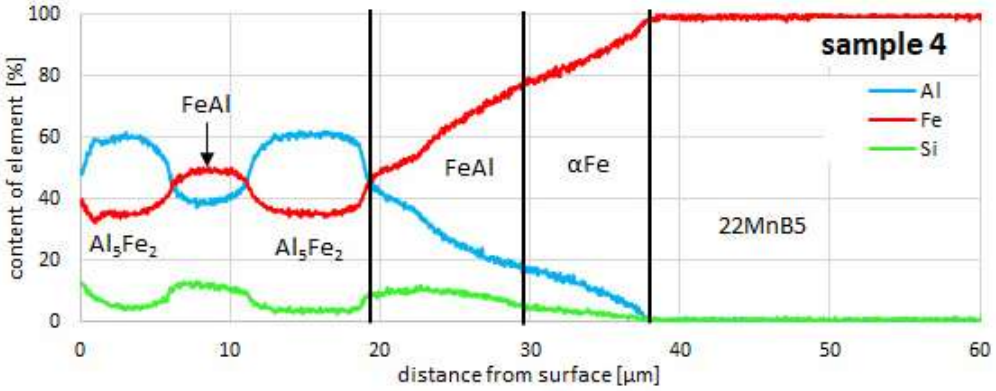

FIGURE 8. Chemical compound in line for sample 4 ($t = 12.9\,\text{min}$, $T = 907\,°\text{C}$).

tempered sample 2 (882 °C) with short holding time (5.8 min), sample with mean values of heat treatment parameters 3 - $T = 905\,°C$, $t = 7.4\,min$, and a high values sample 4 - $T = 907\,°C$, $t = 12.9\,min$.

4. Results and discussion

Figure 1 (left) shows that, before the austenitization, the AlSi coating consists of pure aluminium, the $Al_2Fe_3Si_3$ phase and the Al_8Fe_2Si precipitate on the steel-coating interface. The iron diffusion into the partially molten AlSi coating is very rapid during the first 2 minutes of the austenitisation. Figure 2 shows that, due to a massive diffusion, the Al_8Fe_2Si precipitate was transformed to $Al_5Fe_2 + Al_2Fe_3Si_3$ according to the equation (1), this is in an agreement with the works published by Schmidova [13] and also Windmann [6, 7].

$$Al \rightarrow Al + Al_8Fe_2Si \rightarrow Al_5Fe_2 + Al_2Fe_3Si_3 \rightarrow \rightarrow Al_5Fe_2 + AlFe \quad (1)$$

After a complete transformation of the coating into the intermetallic phases, there is an increased diffusion of Al towards the steel. Due to the opposite direction of the diffusion of Al and Fe and its different velocity, cavities (Kirkendall's pores) start to form on the coating-steel interface after 6 minutes, as it can be seen in Figure 2 – sample 3 and 4.

Figure 1 (in the middle) shows the reduced Modulus E_r. Steel has $E_r = 210 - 250\,GPa$, the coating has $E_r = 100\,GPa$ (therefore, a half). After the coating transformation, the reduced modulus of the coating and steel is at the same value $E_r = 210 - 250\,GPa$ (see Figure 4). On the indentation hardness graphs (see Figure 3), the influence of the type and proportion of the phase volume can be seen. The original tough coating transformed into a brittle $Al_5Fe_2 + Al_2Fe_3Si_3$ + FeAl after the first 2 minutes of the austenitisation. With the increasing temperature and time, the volume of FeAl increased. In all of the hardness matrices in Figure 3, there is an increase of the hardness in the whole volume of the coating on the left. This is probably due to the used measurement method. The XPM is a method with very fast tip crossings between individual indents. After such a transition from the end of the matrix (right) to the beginning of the next row of the matrix (left), the measuring tip can oscillate. Measured values may be up to 2 GPa higher. When comparing the values with the right half of the matrix, we can clearly see the increase in the hardness (orange and red).

In Figures 5 to 8, there are graphs from the linear SEM analysis. The graphs show how incredibly fast the thickness of the diffusion layer (αFe) increases from 0 to up to 10 micrometers during the first 6 minutes. After 6 minutes, its growth slows down and the FeAl layer begins to increase considerably. It can also be observed that the volume of the FeAl phase throughout the coating increases steeply, which corresponds to the results above.

5. Conclusion

The results of the research show that a massive diffusion occurs during the austenitization, which causes the transformation of the original AlSi coating into intermetallic phases of the type $Al_5Fe_2 + Al_2Fe_3Si_3$. After the transformation, the phase spacing does not affect the reduced modulus. With increasing temperature and austenitizing time, the volume of the FeAl + αFe phase in the coating is increasing. This work should be followed by welding tests. Knowing the results of the diffusion processes subsequently related to the quality of the weld joint will allow to determine and limit the heating conditions (thermal processing parameters) before the forming process.

Acknowledgements

This research was supported by the project SGS16/217/OHK2/3T/12.

References

[1] M. Kolaříková, P. Nachtnebl. Properties of interface between manganese-boron steel 22MnB5 and coating Al-Si. In *METAL 2016 - Conference Proceedings*, pp. 735–740. 2016.

[2] Volkswagen Aktiengesellschaft. Tl 4225. alloyed quenched and tempered steel for press quenching - uncoated or precoated: Material requirements for semi-finished products and components, 2012. Internal document.

[3] M. Kolaříková, L. Kolařík, T. Pilvousek, J. Petr. Mechanical properties of Al-Si galvanic coating and its influence on resistance weldability of 22MnB5 steel. *Defect and Diffusion Forum* **368**:82–85, 2016. DOI:10.4028/www.scientific.net/DDF.368.82.

[4] S. Grauer, E. J. F. R. Caron, N. L. Chester, et al. Investigation of melting in the Al–Si coating of a boron steel sheet by differential scanning calorimetry. *Journal of Materials Processing Technology* **216**:89–94, 2015. DOI:10.1016/j.jmatprotec.2014.09.001.

[5] A. Röttger, M. Windmann, W. Theisen. Phase formation at the interface between a boron alloyed steel substrate and an Al-rich coating. *Surface and Coatings Technology* **226**:130–139, 2013. DOI:10.1016/j.surfcoat.2013.03.045.

[6] M. Windmann, A. Röttger, W. Theisen. Formation of intermetallic phases in Al-coated hot-stamped 22MnB5 sheets in terms of coating thickness and Si content. *Surface and Coatings Technology* **246**:17–25, 2014. DOI:10.1016/j.surfcoat.2014.02.056.

[7] U. Füssel, V. Wesling, A. Voigt, E.-C. Klages. Visualisierung der Temperaturentwicklung in der Schweißzone einschließlich der Schweißelektroden über den gesamten zeitlichen Verlauf eines Punktschweißprozesses. *Schweissen und Schneiden* **4**:634–642, 2012.

[8] D. Richard, M. Fafard, R. Lacroix, et al. Carbon to cast iron electrical contact resistance constitutive model for finitie element analysis. *Journal of Materials Processing Technology* **132**:119–131, 2003. DOI:10.1016/S0924-0136(02)00430-2.

[9] Q. Song, W. Zhang, N. Bay. An experimental study determines the electrical contact resistance in resistance welding. *Welding journal* **84**:73–76, 2005.

[10] P. Rogeon, P. Carre, J. Costa, et al. Characterization of electrical contact conditions in spot welding assemblies. *Journal of Materials Processing Technology* **195**:117–124, 2008. DOI:10.1016/j.jmatprotec.2007.04.127.

[11] E. Schmidová, P. Hanus. Weldability of Al-Si coated high strength martensitic steel. *Periodica Polytechnica Transportation Engineering* **41**:127–132, 2013. DOI:10.3311/PPtr.7113.

[12] W.-J. Cheng, C.-J. Wang. Microstructural evolution of intermetallic layer in hot-dipped aluminide mild steel with silicon addition. *Surface and Coatings Technology* **205**:4726–4731, 2011. DOI:10.1016/j.surfcoat.2011.04.061.

[13] H. Springer, A. Kostka, E. J. Payton, et al. On the formation and growth of intermetallic phases during interdiffusion between low-carbon steel and aluminum alloys. *Acta Materialia* **59**(4):1586–1600, 2011. DOI:10.1016/j.actamat.2010.11.023.

[14] J.-G. Yun, J.-H. Lee, S.-Y. Kwak, C.-Y. Kang. Study on the formation of reaction phase to si addition in boron steel hot-dipped in al–7ni alloy. *Coatings* **7**:186, 2017. DOI:10.3390/coatings7110186.

[15] G. Eggeler, W. Auer, H. Kaesche. On the influence of silicon on the growth of the alloy layer during hot dip aluminizing. *Journal of Materials Science* **21**(9):3348–3350, 1986. DOI:10.1007/BF00553379.

[16] U. Köster, W. Liu, H. Liebertz, M. Michel. Mechanical properties of quasicrystalline and crystalline phases in Al-Cu-Fe alloys. *Journal of Non-crystalline Solids* **153-154**:446–452, 1993. DOI:10.1016/0022-3093(93)90393-C.

[17] S. Kobayashi, T. Yakou. Control of intermetallic compound layers at interface between steel and aluminum by diffusion-treatment. *Materials Science and Engineering: A* **338**:44–53, 2002. DOI:10.1016/S0921-5093(02)00053-9.

[18] M. Krasnowski, S. Gierlotka, T. Kulik. Nanocrystalline Al5Fe2 intermetallic and Al5Fe2–Al composites manufactured by high-pressure consolidation of milled powders. *Journal of Alloys and Compounds* **656**:82–87, 2015. DOI:10.1016/j.jallcom.2015.09.224.

[19] A. Kubošová, M. Karlík, P. Haušild, J. Prahl. Fracture behaviour of Fe3Al and FeAl type iron aluminides. *Materials Science Forum* **567-568**:349–352, 2008. DOI:10.4028/www.scientific.net/MSF.567-568.349.

[20] C. Kim, M. J. Kang, Y.-D. Park. Laser welding of Al-Si coated hot stamping steel. *Procedia Engineering* **10**:2226–2231, 2011. DOI:10.1016/j.proeng.2011.04.368.

[21] Y. Shiota, H. Muta, K. Yamamoto, et al. A new semiconductor Al2Fe3Si3 with complex crystal structure. *Intermetallics* **89**:51–56, 2017. DOI:10.1016/j.intermet.2017.05.019.

[22] K. Rokosz, T. Hryniewicz, J. Lukeš, J. Sepitka. Nanoindentation studies and modeling of surface layers on austenitic stainless steels by extreme electrochemical treatments: Nanoindentation and modeling of SL on stainless steels by EP1000. *Surface and Interface Analysis* **47**:643–647, 2015. DOI:10.1002/sia.5758.